Reconstruction of Behind Armour Blunt Trauma Impact Scenarios for Soft Armour Using a Detailed Thorax Model

Duane Cronin, K Rafaels, C Bir, J Barker, D Singh, M Bustamante, P Sathananthan

I. INTRODUCTION

Thoracic response and the potential for injury from the dynamic deformation of protective body armour are challenging to assess because of the focal nature and short duration of the impact. Following a non-penetrating impact, the deformation of protective body armour may impact the thorax, leading to Behind Armour Blunt Trauma (BABT). In a recent study of injuries collected from survivors of body armour impacts, the injuries spanned from minor abrasions and contusions to internal injuries that required medical intervention [1].

Detailed Finite Element (FE) human models can provide insight into the response and potential for injury from BABT impacts [2-3], but require appropriate boundary conditions to represent the impact scenario. There is a paucity of information regarding the time-velocity profile of armour deformation in the literature, and it is essential to include the coupling between the thorax or surrogate and the armour, particularly later in the impact event. The aim of the current study was to reconstruct actual impacts from BABT survivors [1] using experimental test data from similar impacts on clay and a physical test device known as the Blunt Thoracic Trauma Rig (BTTR). The impact scenarios were applied to a previously validated detailed thorax FE model (Fig. 1), and the predicted potential risk for injury was assessed using actual BABT scenarios where the survivors were impacted by a projectile while wearing soft body armour.

II. METHODS

A detailed thorax model, enhanced with high-deformation rate material properties and computationally stable for aggressive impact scenarios, was applied to the reconstruction of BABT impact events (Fig. 1). A mesh refinement study was undertaken using pendulum and non-lethal weapon blunt impact data to validate the thorax response (force-displacement) and to identify an appropriate mesh size for the soft tissues. The final mesh comprised 509,180 solid elements, 71,241 shell elements and 1,129 beam elements.

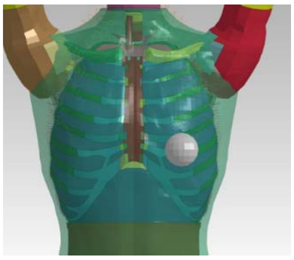

Fig. 1. Thorax FE model and BABT impact condition.

$$V(t) = V_{Peak}\left(1 - \frac{t}{t_0}\right) e^{-\frac{bt}{t_0}}$$

$V(t)$ = Velocity (m/s)
V_{Peak} = Peak Velocity (m/s)
t = time (s)
t_0 = time to zero velocity (s)
b = decay constant (-)

Eq. 1

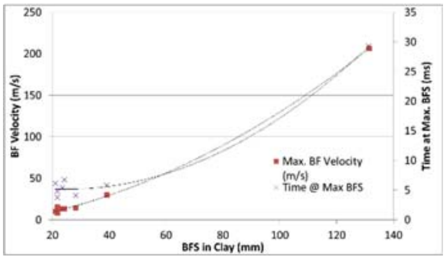

Fig. 2. Correlation for maximum velocity and time at maximum BFS.

Three BABT cases from an existing database, with injuries ranging from minor to severe on the BABT injury rank scale used in Bir *et al*. [1], were identified for reconstruction. Experimental tests on clay were used to determine the BABT impact size and maximum displacement during the event, while the same impacts on a BTTR were used to determine the initial back face velocity and time to maximum displacement for the impact event. The resulting data were represented as a velocity-time history (Eq. 1) [2] and applied to reconstruct three BABT cases from the existing BABT database (Table I). The BABT impact conditions developed in this study were applied using a previously developed prescribed velocity-time methodology [2], using a spherical impactor to represent the behind armour response and interaction with the torso.

D. Cronin (email: dscronin@uwaterloo.ca) is a Professor of Engineering and J. Barker, D. Singh, M. Bustamante, P. Sathananthan are Research Associates, all at the University of Waterloo, Canada. K. Rafaels is an Engineer and Team Leader at the U.S. Army Research Laboratory. C. Bir is a Professor at the University of Southern California.

III. INITIAL FINDINGS

The BTTR and clay impact data [1,4] were assembled for nine impact scenarios with varying projectiles, armours and impact velocities (Fig. 2), and curves were fit to each data set using regression (R^2>0.987). The time to maximum displacement varied from 3.7 m/s to 29.3 m/s, with initial back face velocity ranging from 8 m/s to 206 m/s. The fit curves were used to determine the loading parameters (Eq. 1) for the three reconstruction cases, and the boundary conditions were applied to the thorax model as a prescribed velocity-time curve.

The three BABT impact scenarios (cases 3066, 2576 and 990) were applied to the FE thorax model at the locations identified in the survivor reports and were simulated over a time of 100 ms to ensure the full response of the thorax was captured. Hard tissue failure was determined by element erosion based on a critical plastic strain [5]. The potential for pulmonary contusion was determined using a critical dynamic pressure criterion developed for the FE thorax model [6]. The model predictions (Table I) were generally in good agreement with the reported injuries for the BABT cases.

TABLE I
BABT CASES FOR RECONSTRUCTION AND FE MODEL PREDICTIONS

BABT Survivor Cases and Reconstruction						FE Injury Prediction	
Case (#)	Injury Rank [1] (#)	Reported Injury [3]	Clay BFS (mm)	Maximum BF Velocity (m/s)	Time at BFS (ms)	Rib Fracture (-)	Pulmonary Contusion (% Volume)
3066	1 (minor)	Skin abrasion	21.9	11.0	5.2	None	<0.001 %
2576	2 (moderate)	Fracture, 8th rib	40.4	29.9	5.6	Yes	3.29%
990	3 (severe)	Fracture, 9th rib, lung contusion	65.6	64.8	8.6	Yes	7.96%

IV. DISCUSSION

Combining the data from traditional armour-on-clay tests and newer armour-on-BTTR tests provided appropriate information to define BABT boundary conditions that could be applied to a thorax FE model. The clay test provided post-test measurements of the maximum dynamic deformation of the armour, as well as the size and shape of the impact crater in the clay. It has been noted that the impact crater for hard armour is spherical in shape [2], but this may vary for the soft armour investigated in the current study. The craters for the reconstructed cases were generally spherical, but a more general method will be needed in future to define the shape of the armour deformation. The BTTR data provided an estimate of the initial velocity of the thoracic wall and the time for the maximum deformation to occur. It was noted that the maximum deformation of the BTTR and the Back Face Signature (BFS) in clay were linearly related (R^2=0.997), with the BTTR maximum displacement being smaller than the BFS in clay. This is not unexpected since the BTTR displacement is measured on the rear of the membrane and may potentially attenuate some of the displacement by through-thickness deformation. Also, the compliance of the BTTR membrane and clay are known to differ. However, this effect is anticipated to be most significant at the end of the impact scenario (maximum displacement), where the deformation of the armour may be influenced by the backing medium.

The FE model predictions included thorax response and the potential for injury. Although many challenges have been noted in the literature regarding the prediction of rib fracture, the focal nature of BABT makes the prediction more straightforward. The rib fracture and pulmonary contusion results were in general agreement with the medical records of the survivors; at present, however, minor injuries, such as skin laceration and superficial contusion, are not assessed due to a lack of injury criteria. In the experiments and simulations, the armour was located adjacent to the thorax. There is a known sensitivity of BABT injuries to stand-off and this should be parametrically investigated in the future.

The current study demonstrates the ability to reconstruct a small set of real-world BABT cases using experimental data to define the boundary conditions and a detailed thorax model to assess the potential for injury. Ultimately, this FE tool will enable improved insight into the mechanics of BABT and potential for injury.

V. REFERENCES

[1] Bir, C., *et al*., International Ballistics Symposium, 2017. [2] Cronin, D. S., IRCOBI, 2015. [3] Cronin, D. S., IRCOBI, 2012. [4] Hewins, K., *et al*., Personal Armour Systems Symposium, 2012. [5] Forbes, *et al*., *Int J Crashworthiness*, 2006. [6] Yuen, *et al*., World Congress of Biomechanics, 2010.